ORIGINAL SCIENTIFIC PAPER

CROATICA CHEMICA ACTA

Croat. Chem. Acta **2017**, *90*(2), 207–213
Published online: July 20, 2017
DOI: 10.5562/cca3133

HKD 1926

Graphene Based Composite Hydrogel for Biomedical Applications

Katarina Nešović,[1] Mohamed M. Abudabbus,[1] Kyong Yop Rhee,[2,*] Vesna Mišković-Stanković[1,2,#]

[1] University of Belgrade, Faculty of Technology and Metallurgy, Karnegijeva 4, 11000 Belgrade, Serbia
[2] Department of Mechanical Engineering, Kyung Hee University, 17104 Yongin, South Korea
* Corresponding author's e-mail address: rheeky@khu.ac.kr
# Corresponding author's e-mail address: vesna@tmf.bg.ac.rs

RECEIVED: April 21, 2017 * REVISED: June 21, 2017 * ACCEPTED: June 23, 2017

THIS PAPER IS DEDICATED TO PROF. MIRJANA METIKOŠ-HUKOVIĆ ON THE OCCASION OF HER BIRTHDAY

Abstract: In this work, composite hydrogel consisting of poly(vinyl alcohol), graphene and silver nanoparticles, (Ag/PVA/Gr), was prepared by the immobilization of silver nanoparticles (AgNPs) in PVA/Gr hydrogel matrix in two steps. The first step was cross linking of the PVA/Gr colloid solution by the freezing/thawing method, while in the second step, *in situ* electrochemical method was used to incorporate AgNPs inside the PVA/Gr hydrogel matrix. We used UV–vis spectroscopy, cyclic voltammetry, Raman spectroscopy, DSC analysis, as well as test of cytotoxicity and antibacterial activity, to characterize obtained Ag/PVA/Gr hydrogel. It was shown that graphene-based composite hydrogel with incorporated AgNPs is non toxic biomaterial with antibacterial activity, with a potential for use in biomedical purposes.

Keywords: hydrogels, silver nanoparticles, poly(vinyl alcohol), graphene, nanocomposites, electrochemical synthesis.

INTRODUCTION

IN the light of ever-present need for modernization and improvement of biomedical devices used in treatment of severe wounds and tissue damage, more and more research around the world is dedicated to investigation of novel composites and nanocomposites for medical applications, such as wound dressings and tissue implants.[1–4] Polymers, synthetic or natural, are prevalent foundation of such materials, because of their similarities to real tissue, capability to take on many shapes and forms, and almost immeasurable possibilities to tailor their properties to the unique requirements of target use. Hydrogels based on synthetic and natural polymers or their blends, interpenetrating networks and copolymers, are widely used and researched for biomedical purposes, because of their biocompatibility, hydrophilicity and malleability, which allow relatively easy processing and wide range of applications. Among others, poly(vinyl alcohol) (PVA) is a biocompatible synthetic polymer that has been widely used for preparation of biomedical composite materials, such as wound dressings[5,6] and scaffolds for tissue engineering.[7,8] PVA hydrogels are hydrophilic, containing many hydroxyl groups, which allow them to readily swell in aqueous solutions, thus enabling the regulation of the moisture of the wound surroundings. Cross linking of PVA can be done by simple freezing-thawing method,[9,10] eliminating the need to use toxic cross linkers which could be difficult to remove from the hydrogel. Additionally, PVA is a known stabilizer often used to synthesize and load metal nanoparticles, which bind to –OH groups on the PVA chains and their surface energy is lowered *via* interactions with active sites on polymer chains.[11] Silver nanoparticles (AgNPs) are particularly interesting for use in medical applications, because of their unique and efficient antimicrobial activity against many microorganisms, including bacteria, viruses and eukaryota.[12,13] Graphene (Gr) is a relatively new material that has seen applications in many branches of materials science, from electronic and thermoregulatory devices,[14–16] to biomedical applications.[17,18] As a 2D carbon-atom monolayer, Gr has high mechanical strength and excellent thermal and electrical conductivity,[19,20] which makes it strong candidate for improvement of many properties of compo-

site materials. Indeed, graphene has been reported to improve many physico-mechanical properties of polymer composites, e.g. tensile strength, thermal stability and conductivity.[21,22] By incorporating graphene into the PVA polymer matrix, we attempted to improve specific properties of Ag/PVA/Gr nanocomposite hydrogels with respect to their topical application. The wound dressings for severe wounds are aimed for prolonged use, over the course of several weeks, during which the dressing is supposed to retain most of its mechanical strength, elasticity, exudate absorption ability and antibacterial activity. Graphene, as a nanofiller in PVA hydrogels, has been shown to improve the overall mechanical strength and elasticity of the polymer matrix.[23] This was also confirmed for PVA/Gr and Ag/PVA/Gr nanocomposites in our previous work.[21,24,25] Additionally, several studies indicated that graphene possesses a certain degree of antibacterial activity, with the ability to induce membrane rupture and oxidative stress of bacterial cells.[26,27] This could be an important property, especially in the initial period of Ag/PVA/Gr wound dressing application, when Gr presence could enhance the antibacterial properties of AgNPs and help prevent wound infection and biofilm formation.

The aim of this work was to produce nanocomposite graphene-based biomaterial with incorporated silver nanoparticles using *in situ* electrochemical method, aimed for soft tissue implants, wound dressings and drug delivery. The electrochemical route of nanoparticles synthesis is especially attractive for biomedical applications due to high purity and precise size control of metal particles and the absence of chemical cross linking agents and undesired products.

EXPERIMENTAL

Materials

Ultra-pure Milli-Q water (Millipore, Billerica, MA, USA) is utilized in all syntheses and experiments. The following chemicals are used: poly(vinyl alcohol) powder (fully hydrolyzed, M_w = 70000–100000; "hot soluble"; Sigma Aldrich, St. Louis, MO, USA), silver nitrate (M. P. Hemija, Belgrade, Serbia), potassium nitrate (Centrohem, Stara Pazova, Serbia), graphene powder (Graphene Supermarket, Calverton, NY, USA).

Electrochemical Synthesis of Composite Hydrogel

Electrochemical synthesis of composite Ag/PVA/Gr hydrogel was performed according to the procedure we published elsewhere.[24] In brief, an aqueous solution of the PVA (10 wt%) was prepared by dissolving the PVA powder in hot dH_2O (90 °C). PVA/Gr dispersion was prepared by adding graphene under vigorous stirring, to obtain a final concentration of 10 wt% PVA and 0.01 wt% Gr. After being cooled, the PVA/Gr colloid dispersion was subjected to successive freezing and thawing for five cycles, each of which consisted of freezing at -18 °C for 16 h, and thawing at 4°C for 8 h. The obtained hydrogel was cut into small discs (diameter $d \approx 10$ mm; thickness $\delta \approx 5$ mm) and subjected to swelling for 48 h in a precursor solution containing different concentrations of $AgNO_3$ (0.25, 0.5 or 3.9 mM) and 0.1 M KNO_3 at 25°C. *In situ* electrochemical reduction of Ag^+ at a constant voltage (90 V) was carried out in swollen PVA/Gr hydrogel, to obtain Ag/PVA/Gr nanocomposite with incorporated AgNPs. The hydrogel discs were placed between the two Pt electrodes in the special glass holder. The synthesis was carried out for 4 min, using DC power source MA 8903 Electrophoresis Power Supply (Iskra d.d., Ljubljana, Slovenia).

Methods of characterization

UV-Visible (UV-Vis) spectroscopy. A CARY 300 Bio spectrophotometer (Varian Medical Systems Inc., Palo Alto, CA, USA) was used to record UV-vis spectra in the wavelength range of 200–800 nm.

Raman spectroscopy. High-resolution Raman analysis was carried out using a 514-nm Ar laser Renishaw Invia Raman spectrophotometer (Renishaw plc, UK) in the spectral range from 3500 to 100 cm^{-1}.

Cyclic voltammetry (CV). CV data was acquired using a Reference 600 Potentiostat/Galvanostat/ZRA (Gamry Instruments, USA). Scan rate was 50 $mV \cdot s^{-1}$, starting from the open circuit potential, in the potential range from −0.3 V to 1.0 V vs. SCE.

Field emission scanning electron microscopy (FE-SEM). FE-SEM LEO SUPRA 55 (Carl Zeiss AG, Germany) was used to analyze surface morphology. The instrument was equipped with MIRA 3 XMU (TESCAN, Czech Republic), with In-Lens detector in combined SE/BSE mode, and operated at 10 kV acceleration voltage.

Differential scanning calorimetry (DSC). The DSC measurements were carried out under nitrogen atmosphere on TGA Q5000 IR/SDT Q600 (TA Instruments, USA); temperature range 20–1000°C.

Cytotoxicity. Peripheral blood mononuclear cells (PBMCs) were prepared according to the protocol we published elsewhere.[24] In brief, the experimental procedure involved seeding PBMC suspension in a 24-well plate in nutrient medium. Control was cell suspension without biomaterial samples. PVA/Gr and Ag/PVA/Gr hydrogel samples (2 g) were placed into the 24-well plates, and either PBMC suspension or blank nutrient was added. Tetrazolium dye MTT test was employed for determination of target cell survival. The number of viable cells was assessed based on the change of optical absorbance of MTT treated cells, due to dehydrogenase activity of their mitochondria.[28] The percent of cell survival (*S*) was

calculated using the following equation:

$$S(\%) = \frac{A_u}{A_c} \times 100 \quad (1)$$

where A_u is the absorbance of PBMCs in the presence of Ag/PVA/Gr hydrogel and A_c is the absorbance of control PBMCs. Cytotoxicity of the samples was described according to the following scale, based on the cell viability relative to control: > 90 % survival – non-cytotoxic, 60–90 % survival – slightly cytotoxic, 30–59 % survival – moderately cytotoxic, ≤ 30 % survival – severely cytotoxic.[28,29]

Antibacterial activity. Ag/PVA/Gr hydrogel, obtained from 0.25 mM $AgNO_3$ swelling solution, was tested against Gram-positive *Staphylococcus aureus* TL (culture collection–FTM, University of Belgrade, Serbia) and Gram-negative *Escherichia coli* (ATTCC 25922) bacteria strains. The evaluation of antibacterial activity was carried out using test in suspension, *via* the spread-plate protocol we published elsewhere.[24] The number of viable colonies (CFU mL^{-1}) of *S. aureus* and *E. coli* was determined using a colony counter at the start of the experiment and after incubation at 37 °C for up to 24 h.

RESULTS AND DISCUSSION

Preparation of PVA/Gr hydrogels

Prior to electrochemical synthesis of AgNPs, the PVA/Gr hydrogels were prepared from the colloid dispersions using a simple cyclic freezing-thawing method. It has been long known that PVA colloids, frozen and subjected to subsequent cycles of freezing and thawing, result in the formation of physical, thermo-reversible hydrogels.[30,31] The properties of the obtained hydrogels, such as swelling behavior, elasticity and mechanical strength, depend strongly on the initial colloid concentration, as well as the freezing and thawing temperature, duration and number of cycles.[30] In our work, the freezing parts of the cycles were performed for 16 h at −18 °C, and the thawing temperature was 4 °C in order to allow for a slower thawing process, resulting in a more ordered structure, as opposed to shock-melting at room temperature. Although it is obvious that physical cross linking sites are formed during the preparation of the hydrogel, several mechanisms of gelation *via* the cyclic freezing-thawing technique have been proposed, including intermolecular hydrogen bonding (responsible for the formation of physical cross links), liquid-liquid (LL) and liquid-solid (LS) phase separation.[31–34] LS phase separation is believed to occur *via* diffusion of water and formation of ice crystals during the freezing parts of the cycle, leaving out PVA macromolecules as impurities from the formed ice. After each cycle, the water ice phase and PVA phase become purer and are separated, whereas during thawing process the pores are formed at the sites of ice crystals.[31,34] Finally, LL phase separation is explained by the spinoidal decomposition process during the gelation, leaving polymer-poor and polymer-rich regions, where afterwards gel formation takes place *via* hydrogen bonding.[32] Most probably the formation of PVA/Gr hydrogels is achieved through the combination of aforementioned processes, and well-dispersed graphene remains entrapped in the formed PVA cross linked network. The advantages of the described technique for preparation of PVA hydrogels, especially for biomedical applications, include ability to avoid toxic aldehyde cross linkers, higher mechanical strength than the gels obtained by irradiation cross linking, good elasticity and high swelling degree.[35]

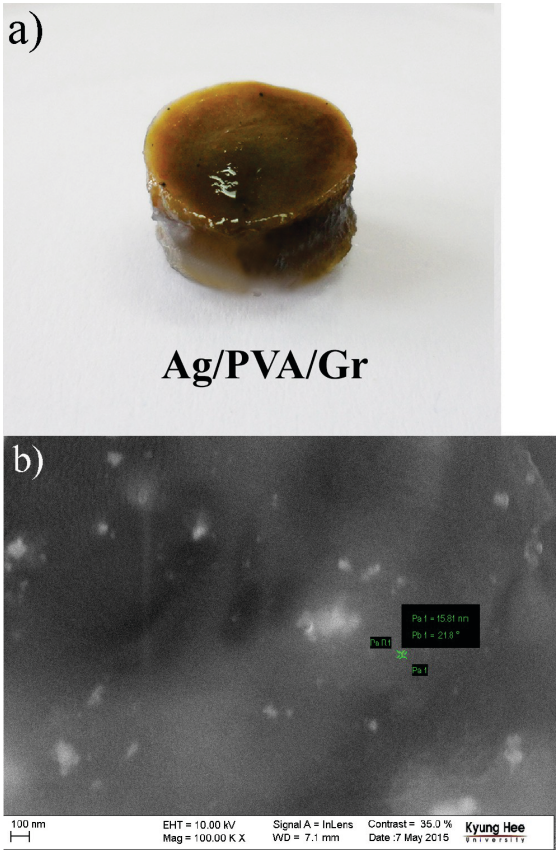

Figure 1. (a) Photograph and (b) FE-SEM microphotograph of Ag/PVA/Gr hydrogel synthesized from 3.9 mM $AgNO_3$ swelling solution.

Electrochemical synthesis

Electrochemical synthesis of AgNPs inside PVA/Gr hydrogel matrix is founded on *in situ* electrochemical reduction of Ag^+ precursor ions in hydrogel disc swollen in 3.9 mM $AgNO_3$ solution prior to synthesis. The reduction was carried at 90 V, during 4 min. The appearance of a dark brown color of Ag/PVA/Gr disc (Figure 1a) is evidence of

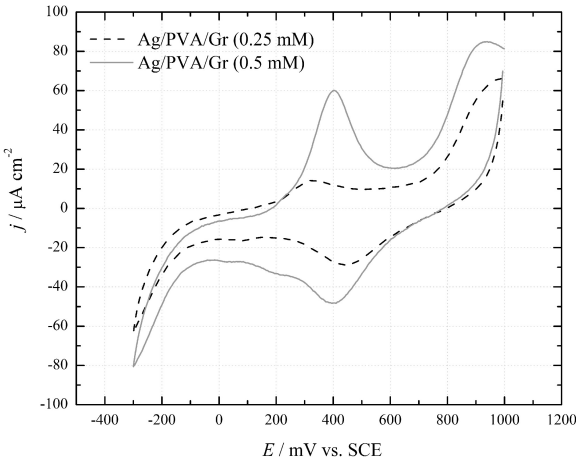

Figure 2. Stationary cyclic voltammograms of Ag/PVA/Gr hydrogels synthesized from 0.25 mM and 0.5 mM $AgNO_3$ swelling solutions; scan rate 50 mV·s^{-1}.

incorporation of AgNPs within PVA/Gr hydrogel. The effect of polymer matrix on stabilization of nanoparticles and hindering the undesired deposition of a silver layer at the cathode surface has been explained elsewhere.[24,36] Namely, –OH groups of PVA chain interact with Ag^+, allowing for the formation of Ag_m^{m+}-PVA complex, which undergoes electrochemical reduction at the cathode surface. Resulting Ag_m^0-PVA complex is then stabilized by PVA chains.

Figure 1b depicts FE-SEM microphotograph of Ag/PVA/Gr hydrogel. The AgNPs are well dispersed inside the polymer matrix of the hydrogel, adopting spherical morphology with dimensions in the nanometer range (10–30 nm). Therefore, the FE-SEM analysis confirmed incorporation of silver nanoparticles in Ag/PVA/Gr nanocomposite hydrogels.

The UV–vis spectrum of Ag/PVA/Gr hydrogels exhibited absorption peak ≈400 nm (data not shown), essentially confirming the formation of AgNPs in the hydrogel matrix. Namely, it is well known that the peak in the 400–420 nm range is characteristic for spherical silver nanoparticles, due to the surface plasmon resonance effect.[37–40] Raman spectroscopy verified incorporation of graphene by appearance of characteristic bands at 1370 cm^{-1} (Raman D-band) and 1580 cm^{-1} (G-band).[24]

Cyclic Voltammetry

Cyclic voltammetry was employed in order to investigate the redox processes of the Ag/PVA/Gr hydrogels on the surface of Pt electrodes. Figure 2 represents stationary voltammograms (CVs which are acquired after several cycles and remain unchanged in subsequent cycles) of Ag/PVA/Gr hydrogels obtained from $AgNO_3$ swelling solutions with two concentrations of Ag^+ (0.25 mM and 0.5 mM). In the anodic sweep, both CVs contain one prominent peak, at 345 mV for Ag/PVA/Gr

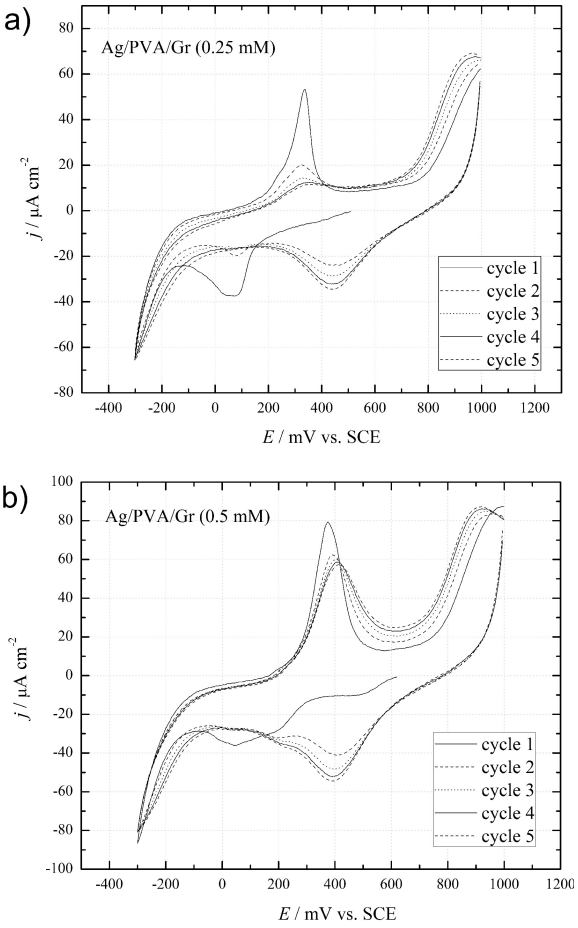

Figure 3. Cyclic voltammograms of Ag/PVA/Gr hydrogels synthesized from (a) 0.25 mM and (b) 0.5 mM $AgNO_3$ swelling solutions; scan rate 50 mV·s^{-1}.

from 0.25 mM $AgNO_3$, and at 405 mV for Ag/PVA/Gr from 0.5 mM $AgNO_3$. These peaks can be ascribed to the oxidation of silver nanoparticles from the hydrogel on the surface of Pt electrode.[25,41] Since the anodic current density of a peak in cyclic voltammograms is proportional to the concentration of the reactive species, it is evident from Figure 2 that Ag/PVA/Gr obtained from 0.5 mM $AgNO_3$ swelling solution contains nearly six times higher amount of AgNPs than Ag/PVA/Gr from 0.25 mM $AgNO_3$, indicating more successful synthesis of Ag/PVA/Gr from 0.5 mM $AgNO_3$. Another anodic process occurs at potentials more positive than 800 mV, seen as a shoulder with high current densities on the CVs. This potential region covers oxygen evolution reaction and formation of surface oxides on the Pt electrode,[42,43] but here is also possible formation of higher oxides of silver. The cathodic sweep contains a broad peak at 430 mV for Ag/PVA/Gr from 0.25 mM $AgNO_3$, and at 395 mV for Ag/PVA/Gr from 0.5 mM $AgNO_3$, which is ascribed to the reduction reaction of Pt and Ag oxides, formed in the anodic sweep.

Figure 3 depicts five cyclic voltammetric sweeps of Ag/PVA/Gr hydrogels obtained from 0.25 mM (Figure 3a) and 0.5 mM (Figure 3b) $AgNO_3$ swelling solutions. Voltammograms of both hydrogels quickly reach steady state after several cycles. During cycles 1–5, a continuous decrease of the anodic current density can be observed for the peak of oxidation of AgNPs at 320–340 mV for Ag/PVA/Gr from 0.25 mM $AgNO_3$, and at 370–390 mV for Ag/PVA/Gr from 0.25 mM $AgNO_3$, followed by an increase in current density of oxygen evolution peak at potentials higher than 700 mV for both hydrogels. The major differences are between the first and subsequent cycles, indicating that polymer/Pt interface is quickly depleted of AgNPs and there is a much smaller amount available for oxidation in the subsequent scans. In the cathodic region for both hydrogels, cycle 1 contains peaks at ~ 50 mV, which probably involve reduction of residual Ag^+ ions, remaining unreduced in the hydrogel after the synthesis. The disappearance of this peak in cycles 2–5 hints that almost all Ag^+ ions are reduced in the first cycle of the CV sweep.

DSC Measurements

The DSC thermograms of both PVA/Gr (as reference) and Ag/PVA/Gr hydrogels exhibit endothermic changes in the range of 20–1000 °C (Figure 4). The first endothermic peak, at 119 °C for PVA/Gr and at 120 °C for Ag/PVA/Gr, is related to the evaporation and loss of water from the hydrogel network upon heating the samples. The high temperature of this event (~ 120 °C) indicates that water molecules are strongly hydrogen bonded to the hydroxyl groups on the PVA chain, as well as to oxidized groups in graphene structure. This is bound water with highly oriented and ordered dipoles that usually evaporates at higher temperatures.[44] The area of this peak does not change significantly upon addition of Ag to PVA/Gr hydrogel, which implies that AgNPs have small influence on the binding and orientation of H_2O molecules in the polymer matrix. The loss of free water at temperatures lower than 100 °C did not result in any significant peaks on both DSC curves, so we conclude that the main state of water in hydrogels is bound H_2O, due to the presence of a large number of oxygen-containing groups in PVA macromolecules.

The second endothermic peak on DSC curves of PVA/Gr and Ag/PVA/Gr is located at 287 °C and 311 °C, respectively, and is related to the melting of the polymer. The melting point, T_m, of pure PVA is reported to be in the range of 200–220 °C.[45–47] T_m of PVA/Gr hydrogel is shifted to significantly higher temperatures (287 °C) with respect to PVA, indicating increased thermal stability due to incorporated graphene. Graphene and graphene-oxide nanofillers are known to improve thermal properties of polymer materials, often owing to the incorporation inside the hydrogel structure, as well as interactions with polymer

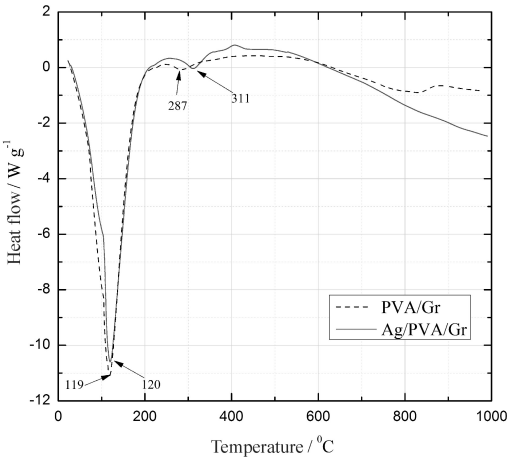

Figure 4. DSC curves of PVA/Gr and Ag/PVA/Gr hydrogels (swelling solution: 3.9 mM $AgNO_3$).

chains that lead to lowered mobility and higher stability of the polymer matrix. It is well known that graphene always possesses a certain amount of oxygen-containing groups, present as impurities or residues from the manufacturing process, which allow it to be dispersed in aqueous media and form bonds with various materials. The interactions with PVA are achieved *via* hydrogen bonding between these oxygenated groups of graphene, and –OH groups of PVA. Several studies have shown the influence of graphene fillers on thermal stability and thermal degradation of polymeric networks, such as poly(methyl methacrylate) (PMMA),[48,49] PVA films[23] and PVA/starch blends.[50,51]

Furthermore, melting of Ag/PVA/Gr hydrogel occurs at even higher T_m = 311 °C, exhibiting much better thermal stability due to presence of AgNPs together with graphene. This corroborates the assumption that AgNPs form complexes mainly with –OH groups of PVA macromolecule, which has a strong influence on both thermal stability and crystallinity of PVA polymer.

Finally, at temperatures higher than 400 °C, the DSC curves exhibit stable endothermic regions with small change over the analyzed temperature range. This region of the curve probably covers mostly slow thermal oxidation of graphene sheets incorporated in the hydrogels, as also seen by small-area endothermic peak on the DSC curve of PVA/Gr at around 825 °C.

Biological Properties

Although more silver nanoparticles (AgNPs) are synthesized in the hydrogel swollen in 0.5 mM $AgNO_3$, we chose the lowest concentration of silver (0.25 mM) for biological evaluation, in order to prove that our nanocomposite Ag/PVA/Gr hydrogels possess antibacterial properties even with lowest AgNPs content. Moreover, in our previous research,[24,25] we found that hydrogels synthesized from

0.25 mM $AgNO_3$ exhibited good antibacterial activity, at the same time having the mildest cytotoxic effect, which is important for the application of these materials as topical wound dressings. Silver is well known to exhibit dose-dependent toxicity, therefore it is important to achieve desired antibacterial effect, while maintaining low cytotoxicity of the materials based on silver nanoparticles. We found that minimum inhibitory concentration (MIC) of AgNPs towards bacteria with no cytotoxic influence on live human cells is 0.25 mM.[24] At this concentration, AgNPs pose no threat to live human tissue, while still being effective in suppressing bacterial infection.

Peripheral blood mononuclear cells (PBMCs) were chosen for cytotoxicity tests because they represent some of the main populations of leukocytes (lymphocytes, monocytes). In the human immune system, leukocytes manifest first response to infections and inflammations, thus they are relevant indicators of the toxicity of medical devices. Using MTT test of cytotoxicity and Equation (1), the survival, *S*, of PBMCs exposed to Ag/PVA/Gr hydrogel synthesized from 0.25 mM $AgNO_3$ was calculated to be 69.39 %,[24] proving this biomaterial as slightly cytotoxic following the cytotoxicity scale.[28,29]

The antibacterial activity of Ag/PVA/Gr hydrogels was tested against pathogenic microorganisms, *Staphylococcus aureus* (Gram-positive bacterium) and *Escherichia coli* (Gram-negative bacterium),[24] some of the most frequent causes of hospital infections. Calculations based on the initial number of cells (7.80×10^4 CFU mL^{-1} *S. aureus* and 9.0×10^4 CFU mL^{-1} *E. coli*) and 1 h post-incubation (30 CFU mL^{-1} *S. aureus* and 0 CFU mL^{-1} *E. coli*) revealed that Ag/PVA/Gr caused reduction of both bacteria (*S. aureus* TL 97 % cell reduction and *E. coli* complete reduction), exhibiting strong antibacterial activity and potential for antibacterial medical devices.

The antibacterial activity of Ag/PVA/Gr hydrogels can be explained by the release of antibacterial agent – silver nanoparticles. The toxicity of silver towards pathogenic microorganisms is well known, however several mechanisms of action have been proposed, including inhibition of DNA replication, disruption of cell membrane function and respiratory enzymes, all eventually leading to cell death.[52,53] Moreover, AgNPs possess stronger antibacterial activity compared to silver salts and ions, due to large surface area-to-volume ratio and the ability to attach and accumulate on the cell wall,[53] as well as to penetrate the inner membrane and cause the leakage of the cellular material.[54] Additionally, AgNPs release Ag^+ ions, which have antibacterial effect in their own capacity, strengthening the toxic influence of AgNPs on bacteria cells.[52] Ag/PVA/Gr hydrogels were shown to have the ability to release silver over prolonged period of time, with burst release during the first couple of days followed by gradual release over several weeks.[24,25] In such a way, Ag/PVA/Gr hydrogel wound dressings can provide strong protection of the wound against infection and prevent biofilm formation upon initial application, but could also serve as part of antibacterial devices for prolonged use *via* slow release of AgNPs.

CONCLUSION

Prior to electrochemical synthesis of silver nanoparticles (AgNPs), the PVA/Gr hydrogel was obtained from PVA/Gr colloid solution by cross linking using the freezing-thawing method. Then, we successfully incorporated AgNPs into the PVA/Gr hydrogel using an *in situ* electrochemical method of silver ion reduction inside the PVA/Gr matrix at constant voltage of 90 V. Incorporation of AgNPs was confirmed by UV-Vis, CV and FE-SEM, while Raman spectroscopy verified the Gr in the Ag/PVA/Gr hydrogel. MTT test of cytotoxicity proved Ag/PVA/Gr hydrogel as slightly cytotoxic, while strong antimicrobial activity was found against *Staphylococcus aureus* and *Escherichia coli* strains. After only 1 h of incubation, Ag/PVA/Gr caused reduction in viability of both bacteria, *S. aureus* (97 % reduction) and *E. coli* (complete reduction).

Acknowledgment. The authors would like to thank Ministry of Education, Science, and Technology of Korea (Basic Science Research Program grant, contract No. 2016R1A2B4016034) and Ministry of Education, Science, and Technological Development of the Republic of Serbia (contract No. III 45019) for financial support.

REFERENCES

[1] L. Fan, H. Yang, J. Yang, M. Peng, J. Hu, *Carbohydr. Polym.* **2016**, *146*, 427.
[2] S. G. Jin, A. M. Yousaf, K. S. Kim, D. W. Kim, D. S. Kim, J. K. Kim, C. S. Yong, Y. S. Youn, J. O. Kim, H. G. Choi, *Int. J. Pharm.* **2016**, *501*, 160.
[3] W. Mozalewska, R. Czechowska-Biskup, A. K. Olejnik, R. A. Wach, P. Ulański, J. M. Rosiak, *Radiat. Phys. Chem.* **2017**, *134*, 1.
[4] T. Song, S. Tanpichai, K. Oksman, *Cellulose* **2016**, *23*, 1925.
[5] A. Kumar, M. Jaiswal, *J. Appl. Polym. Sci.* **2016**, *133*, 43260.
[6] D. Zhang, W. Zhou, B. Wei, X. Wang, R. Tang, J. Nie, J. Wang, *Carbohydr. Polym.* **2015**, *125*, 189.
[7] K. Kanimozhi, S. Khaleel Basha, V. Sugantha Kumari, *Mater. Sci. Eng. C* **2016**, *61*, 484.
[8] S. H. Oh, D. B. An, T. H. Kim, J. H. Lee, *Acta Biomater.* **2016**, *35*, 23.
[9] N. A. Peppas, Y. Huang, M. Tores-Lugo, J. H. Ward, J. Zhang, *Annu. Rev. Biomed. Eng.* **2000**, *2*, 9.

[10] T. Puspitasari, M. L. Raja, K, D. S. Pangerteni, A. Patriati, E. G. R. Putra, *Procedia Chem.* **2012**, *4*, 186.
[11] K.-S. Chou, C.-Y. Ren, *Mater. Chem. Phys.* **2000**, *64*, 241.
[12] V. Alt, T. Bechert, P. Steinrucke, M. Wagener, P. Seidel, E. Dingeldein, E. Domann, R. Schnettler, *Biomaterials* **2004**, *25*, 4383.
[13] C. Lok, C. Ho, R. Chen, Q. He, W. Yu, H. Sun, P. K. Tam, J. Chiu, C. Che, *J. Biol. Inorg. Chem.* **2007**, *12*, 527.
[14] S. Hertel, D. Waldmann, J. Jobst, A. Albert, M. Albrecht, S. Reshanov, A. Schöner, M. Krieger, H. B. Weber, *Nat. Commun.* **2012**, *3*, 957.
[15] M. F. El-Kady, V. Strong, S. Dubin, R. B. Kaner, *Science* **2012**, *335*, 1326.
[16] Y. F. Zhang, D. Han, Y. H. Zhao, S. L. Bai, *Carbon* **2016**, *109*, 552.
[17] Y. Y. A. M. A. Z. T. D. D. Y. Lin, *Mater. Today* **2013**, *16*, 365.
[18] S. Goenka, V. Sant, S. Sant, *J. Control. Release* **2014**, *173*, 75.
[19] A. Balandin, S. Ghosh, W. Bao, I. Calizo, D. Teweldebrhan, F. Miao, C. N. Lau, *Nano Lett.* **2008**, *8*, 902.
[20] N. O. Weiss, H. Zhou, L. Liao, Y. Liu, S. Jiang, Y. Huang, X. Duan, *Adv. Mater.* **2012**, *24*, 5782.
[21] R. Surudžić, A. Janković, M. Mitrić, I. Matić, Z. D. Juranić, L. Živković, V. Mišković-Stanković, K. Y. Rhee, S. J. Park, D. Hui, *J. Ind. Eng. Chem.* **2016**, *34*, 250.
[22] J. M. Yang, S. A. Wang, *J. Memb. Sci.* **2015**, *477*, 49.
[23] J. Liang, Y. Huang, L. Zhang, Y. Wang, Y. Ma, T. Cuo, Y. Chen, *Adv. Funct. Mater.* **2009**, *19*, 2297.
[24] M. M. Abudabbus, I. Jevremović, A. Janković, A. Perić-Grujić, I. Matić, M. Vukašinović-Sekulić, D. Hui, K. Y. Rhee, V. Miskovic-Stankovic, *Compos. Part B* **2016**, *104*, 26.
[25] R. Surudzić, A. Janković, N. Bibić, M. Vukašinović-Sekulić, A. Perić-Grujić, V. Mišković-Stanković, S. J. Park, K. Y. Rhee, *Compos. Part B Eng.* **2016**, *85*, 102.
[26] S. Liu, T. H. Zeng, M. Hofmann, E. Burcombe, J. Wei, R. Jiang, J Kong, Y. Chen, *ACS Nano*, **2011**, *5*, 6971.
[27] S. Gurunathan, J. W. Han, A. A. Dayem, V. Eppakayala, J. H. Kim, *Int. J. Nanomedicine* **2012**, *7*, 5901.
[28] Ž. Jovanović, A. Radosavljević, Z. Kačarević-Popović, J. Stojkovska, A. Perić-Grujić, M. Ristić, I. Z. Matić, Z. D. Juranić, B. Obradovic, V. Mišković-Stankovic, *Colloid. Surface. B* **2013**, *105*, 230.
[29] G. Sjögren, G. Sletten, J. E. Dahl, *J. Prosthet. Dent.* **2000**, *84*, 229.
[30] S. R. Stauffer, N. A. Peppas, *Polymer* **1992**, *33*, 3932.
[31] N. A. Peppas, S. R. Stauffer, *J. Control. Release* **1991**, *16*, 305.
[32] K. Kawanishi, M. Komatsu, T. Inoue, *Polymer* **1987**, *28*, 980.
[33] W. Stoks, H. Berghmans, **1988**, *20*, 361.
[34] F. Yokoyama, I. Masada, K. Shimamura, T. Ikawa, K. Monobe, *Colloid Polym Sci* **1986**, *264*, 595.
[35] C. M. Hassan, N. A. Peppas, *Biopolym. PVA Hydrogels, Anionic Polym. Nanocomposites* **2000**, *153*, 37.
[36] B. Yin, H. Ma, S. Wang, S. Chen, *J. Phys. Chem. B* **2003**, *107*, 8898.
[37] Ž. Jovanović, A. Radosavljević, M. Šiljegović, N. Bibić, V. Mišković-Stanković, Z. Kačarević-Popovic, *Radiat. Phys. Chem.* **2012**, *81*, 1720.
[38] Ž. Jovanović, J. Stojkovska, B. Obradović, V. Mišković-Stanković, *Mater. Chem. Phys.* **2012**, *133*, 182.
[39] A. Slistan-Grijalva, R. Herrera-Urbina, J. F. Rivas-Silva, M. Avalos-Borja, F. F. Castillon-Barraza, A. Posada-Amarillas, *Phys. E* **2005**, *25*, 438.
[40] A. Slistan-Grijalva, R. Herrera-Urbina, J. F. Rivas-Silva, M. Avalos-Borja, F. F. Castillon-Barraza, A. Posada-Amarillas, *Phys. E* **2005**, *27*, 104.
[41] Z. Jovanovic, A. Radosavljević, J. Stojkovska, B. Nikolić, B. Obradović, Z. Kacarevic-Popovic, V. Miskovic-Stankovic, *Polym. Compos.* **2014**, *35*, 217.
[42] B. E. Conway, *Prog. Surf. Sci.* **1995**, *49*, 331.
[43] D. Gilroy, B. E. Conway, *Can. J. Chem.* **1968**, *46*, 875.
[44] T. Wang, S. Gunasekaran, *J. Appl. Polym. Sci.* **2006**, *101*, 3227.
[45] S. R. Sudhamani, M. S. Prasad, K. Udaya Sankar, *Food Hydrocoll.* **2003**, *17*, 245.
[46] N. A. Peppas, E. W. Merrill, *J. Appl. Polym. Sci.* **1976**, *20*, 1457.
[47] H. Feng, Z. Feng, L. Shen, *Polymer* **1993**, *34*, 2516.
[48] S. Villar-Rodil, J. I. Paredes, A. Martínez-Alonso, J. M. D. Tascón, *J. Mater. Chem.* **2009**, *19*, 3591.
[49] T. Ramanathan, A. A. Abdala, S. Stankovich, D. A. Dikin, M. Herrera-Alonso, R. D. Piner, D. H. Adamson, H. C. Schniepp, X. Chen, R. S. Ruoff, eS. T. Nguyen, I. A. Aksay, R. K. Prud'homme, L. C. Brinson, *Nat. Nanotechnol.* **2008**, *3*, 327.
[50] J. Jose, M. A. Al-Harthi, M. A. A. AlMa'adeed, J. B. Dakua, S. K. De, *J. Appl. Polym. Sci.* **2015**, *132*, 1.
[51] R. Li, C. Liu, J. Ma, *Carbohydr. Polym.* **2011**, *84*, 631.
[52] M. Rai, A. Yadav, A. Gade, *Biotechnol. Adv.* **2009**, *27*, 76.
[53] S. Prabhu, E. K. Poulose, *Int. Nano Lett.* **2012**, *2*, 32.
[54] W. R. Li, X. B. Xie, Q. S. Shi, H. Y. Zeng, Y. S. Ou-Yang, Y. Ben Chen, *Appl. Microbiol. Biotechnol.* **2010**, *85*, 1115.